

TRANSITIONS AND PHENOMENOLOGY OF α,α -TREHALOSE POLYMORPHS INTER-CONVERSION

*F. Sussich and A. Cesàro**

Department of Biochemistry, Biophysics and Macromolecular Chemistry, University of Trieste
Via Giorgieri 1, I-34127 Trieste, Italy

(Received May 2, 2000)

Abstract

The thermal transitions of α,α -trehalose polymorphs have been carefully studied by differential scanning calorimetry (DSC) at different scan rates. Attention has been paid to the correlation of the thermal data with the proper crystalline forms (when present), in order to attribute the observed transitions correctly. In particular, the subtle dehydration process of dihydrate trehalose has been already shown to produce several species, depending on the experimental conditions.

Thermodynamic data (i.e., temperatures and enthalpies) for all the known transitions are reported and the results are critically discussed.

Keywords: α,α -trehalose polymorphs, dehydration, thermodynamics

Introduction

It is widely recognized that the glassy state and crystalline polymorphs play highly important roles. In particular, scientists' attention has been drawn to the properties and transformations involving sugar molecules in the glassy and amorphous states [1, 2] to explain their important functions in food and pharmaceutical formulations. In fact, the peculiar properties of amorphous sugars are believed to lie at the basis of the most widespread applications [3–5]. As a consequence, transition temperatures related to the glassy–amorphous states and to the crystalline–liquid states have been considered to be the first quantitative step in defining the stability of these systems. However, intriguing polymorphic transformations have often hampered the accurate determination of thermodynamic data as well as a proper definition of these transitions, and, as a result, a full understanding of the stability of several crystalline and amorphous phases and their interplay has yet to be found. In particular, an attempt at rationalizing the thermal behavior of trehalose polymorphic forms would be very welcome, given the repeated efforts to produce new data for the elucidation of its protective action against biological deterioration of living microorganisms [6–8]. Our

* Author to whom all correspondence should be addressed.

previous work concentrated on the characterization of the polymorphic states of trehalose, identified by differential scanning calorimetry (DSC), microscopy and X-ray powder diffraction analysis [9–11]. In view of new findings from our laboratory, we wish to re-examine some of the literature data on the transformations of trehalose dihydrate and its anhydrous crystalline polymorphs. Our aim is to assess the dependence of thermodynamic parameters and transformation path upon some experimental variables, being heating rate the most important one.

Experimental

Materials

Dihydrate trehalose (TRE_h) was purchased from Sigma Chemical Co. and was used without further purification. The anhydrous crystalline forms, TRE_α and TRE_β , were prepared by following the procedure described by Perlin and co-workers for their 'a' and 'b' anhydrous forms, keeping the dihydrate samples for four hours at 85°C under vacuum and for four hours at 130°C, respectively. A third crystalline form, TRE_γ , was prepared directly in the calorimeter: dihydrate trehalose was heated up above the endotherm corresponding to dehydration and the scan was stopped at exactly the subsequent cold crystallization, at a temperature around 115°C; the sample was then quenched to room temperature. Details about the different polymorphs and their characterization have already been reported [10, 11].

Calorimetric measurements

Calorimetric measurements were carried out with a Perkin Elmer DSC 7 (power compensation) differential scanning calorimeter, connected to a computer via a TAC7/DX Thermal Analysis Instrument Controller, and Perkin Elmer Pyris Software 3.01s was used. The thermal unit was refrigerated with an external thermocryostat in which the coolant was kept at 0°C; a nitrogen flux was purged through the furnace (flow rate=20 mL min⁻¹). The instrument was calibrated using indium and zinc under the same conditions (scan rate) used in the experiments, according to the standard procedures recommended for standardization and calibration studies. Trehalose samples were placed in aluminum Perkin Elmer DSC pans and sealed with a pierced lid.

Results

Survey of literature data on the melting of trehalose crystals

Before reporting on our experimental results, it is necessary to give a summary of the literature data concerning the melting of anhydrous crystals and the dehydration of dihydrate crystals, called here TRE_β and TRE_h , respectively (Table 1).

Table 1 Literature values for transition temperatures ($^{\circ}\text{C}$) of trehalose (first line gives a schematic definition of the transition involved)

Transition \rightarrow Reference \downarrow	Glass trans./ $^{\circ}\text{C}$	Dehydration $\text{TRE}_h \rightarrow \text{anhydrous}/^{\circ}\text{C}$	Melting of TRE_α $\text{TRE}_\alpha \rightarrow \text{TRE}_a/^{\circ}\text{C}$	Melting of TRE_α $\text{TRE}_\beta \rightarrow \text{TRE}_L/^{\circ}\text{C}$
Reisener (1962)		100 \pm 3		216–218
Shafizadeh (1973)	133**	100**	135** (?)	215**
Green (1989)	79	94*		
Slade (1992)	79			203*
Roos (1993)	100*, 107**	91*, 97**		
Ding (1996)	115			
Sussich (1998)	120*	100–110**	126**	215**

*onset temperature

**mid-point (or peak) temperature

The first report on trehalose transitions was that of Reisener *et al.* [12]. These authors observed, at 100 \pm 3 $^{\circ}\text{C}$, a sintering and birefringence loss of TRE_h , while melting occurred at 135 $^{\circ}\text{C}$. The melting of the anhydrous form TRE_β (prepared at $T > 130^{\circ}\text{C}$) occurred at 216–218 $^{\circ}\text{C}$. They also reported the preparation of another crystalline form, called TRE_α here. These literature values have been quoted by Sussich *et al.* [10] and in a recent survey mostly devoted to the supplemented phase diagram [13].

Shafizadeh and Susott [14] reported DSC curves showing two sharp endotherms at 100 and 215 $^{\circ}\text{C}$, for the melting of TRE_h and TRE_β , respectively. However, their curves (at 5–15 K min^{-1}) showed more endothermic peaks, the complexity of which was attributed to the presence of amorphous glass which undergoes liquification.

In his review on melting and glass transitions of low molecular mass carbohydrates, Roos [15] gave the following data on melting temperatures: onset and peak temperatures of melting are 91 and 97 $^{\circ}\text{C}$, respectively, for the dihydrate crystal, while the onset temperature of 203 $^{\circ}\text{C}$, given for the final melting of the anhydrous TRE_β , was taken from Slade and Levine's data [16]. The value of 100 $^{\circ}\text{C}$ was reported in a subsequent paper [17] as a T_g value (indeed!), with the relevant information that, when rapidly cooled to -100°C , solutions containing from 70 to 90% of sugar were unable to show glass transition upon re-heating. Rapid crystallization of hydrate form was inferred. Green and Angell [18] reported that the melting transition of trehalose dihydrate occurred in the range 90–100 $^{\circ}\text{C}$ (Fig. 1 of [18]), while in a subsequent paper [19] a small endothermic peak at 125 $^{\circ}\text{C}$ was observed for the first scan after dehydration and was attributed to an anomalous glass transition (the doubt over a possible metastable state was also mentioned). Sussich *et al.* [10] prepared the different polymorphs and studied the transformations by DSC, microscopy and X-rays powder diffraction. In addition to the dehydration of TRE_h (100–110 $^{\circ}\text{C}$) and melting of TRE_β (215 $^{\circ}\text{C}$), they reported on the melting of two forms, TRE_α (126 $^{\circ}\text{C}$) and TRE_γ (118–122 $^{\circ}\text{C}$). The latter was then characterized as a mixture of two crystalline forms, and probably made up of TRE_h crystals encapsulated in layers of TRE_β .

Comparison of the different literature data reported in Table 1 is therefore difficult, not only because of the different setups (when reported), but also on account of the difficulty of assigning unambiguously the transition temperature to a defined transformation. In the following results, each trehalose crystalline form was prepared and characterised in advance by X-ray powder diffraction so as to correspond to the polymorphs already reported in our previous work [10, 11].

Influence of temperature scan rate on dehydration profile of TRE_h

Several scan rates were used to follow the DSC profile of the dehydration process of trehalose dihydrate, TRE_h . While in a previous work [11] attention was mainly focused on the transformation pattern for each trehalose polymorph, here the thermodynamics of the dehydration process was carefully examined. The reported data on the characteristic transition of TRE_h were therefore studied in order to understand the prerequisites for water removal.

Dehydration temperatures of TRE_h are reported in Fig. 1a as a function of the scan rate. After a rapid increase of the peak temperature at low scan rates, there is a clear downward curvature with the minimum located at about $10\text{--}20\text{ K min}^{-1}$. More interestingly, a plot of dehydration temperatures as a function of the logarithm of scan rates clearly identifies three different regimes (Fig. 1b), with a parallel trend for very low and very high scan rates and a plateau for the intermediate region of scan rates ($2\text{--}20\text{ K min}^{-1}$). We shall see below that this intermediate range of scan rates produces the formation of a particular morphology of partially dehydrated crystals, previously called TRE_v [10, 11]. It can therefore be inferred that, under the experimental conditions given by the scan rates, the dehydration process occurs with different mechanisms.

In the above phenomenological description of the results, it was a necessary, although arbitrary, choice to report all temperatures as peak temperatures. This deci-

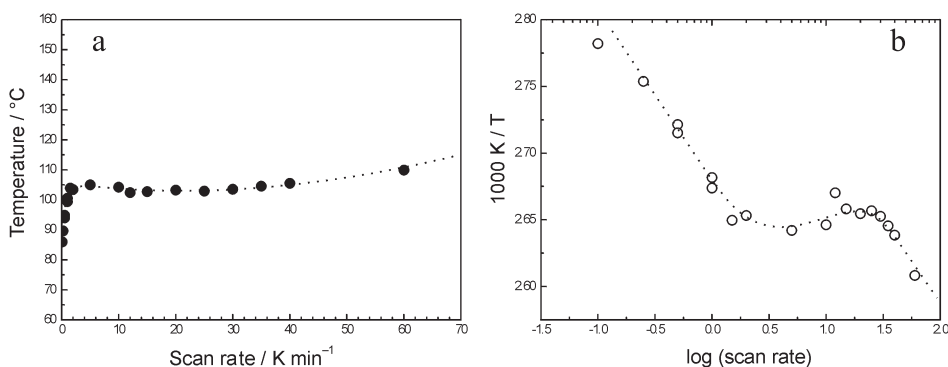


Fig. 1 Dehydration temperature (peak temperature) of TRE_h as a function of the scan rate (a); Dependence of the inverse of dehydration temperature of TRE_h as a function of the logarithm of scan rate: three different regimes are evident (b)

sion was suggested by the fact that the shape of the peaks was not constant and large errors would have occurred in the determination (when possible) of the onset value.

A more correct procedure for the determination of onset temperatures was, however, followed for the values given in the summary (Table 2). As an example, taking the changes in the broadness of the dehydration peak into account, a value of $100 \pm 0.5^\circ\text{C}$ can be obtained as the onset temperature of the dehydration process for scan rates of $10\text{--}40\text{ K min}^{-1}$.

Table 2 Summary of thermodynamic data for trehalose transitions

Transition	$T_{\text{tr}}/\text{K } (^\circ\text{C})^*$	$\Delta H/\text{kJ mol}^{-1}$	$\Delta S/\text{J K}^{-1} \text{ mol}^{-1}$
Dehydration of TRE_h $\text{TRE}_h \rightarrow \text{anhydrous}$	373 (100) ± 0.5	113.5 (full)**	304**
Melting of TRE_α $\text{TRE}_\alpha \rightarrow \text{TRE}_{\text{am}}$	394 (120.9) ± 1.3	5.8 ± 0.3	14.7
Transition of TRE_γ $\text{TRE}_\gamma \rightarrow \text{TRE}_\beta$	385 (111.8) ± 1	33.1 ± 2.5	86
Melting of TRE_β $\text{TRE}_\beta \rightarrow \text{TRE}_l$	479.9 (206.8) ± 0.1	50.0 ± 2	104

*onset temperature

**including two water molecules undergoing vaporization

Trehalose alpha

TRE_α is one of the anhydrous crystalline forms that can be prepared from dihydrate trehalose. Its formation, starting from dihydrate crystals was first described by Perlin and co-workers [12] although new routes for its preparation have also been explored (Sussich *et al.* in preparation). The crystals of TRE_α , heated with scan rates ranging from 1 to 20 K min^{-1} , give rise to DSC curves (Fig. 2a) that display a series of similar features: an endothermic peak arises around 125°C and is followed by a cold crystallization and then by a second endothermic process above 200°C . The first peak is attributed to the melting of TRE_α producing an amorphous phase; at higher temperature the 'cold' crystallization toward TRE_β can be seen, as it is very common for high molecular mass polymers. Being a kinetic phenomenon, the intensity and sharpness of the exothermic peak of cold crystallization depend on scan rate. In addition, the amount of crystals formed depends on the time allowed for crystallization, that is the scan rate. Furthermore, it must be noted that cold crystallization temperatures are very close to the melting temperatures of the crystals produced (TRE_β), because only at high temperatures does the viscosity of amorphous state decrease enough to allow crystal growth. As a consequence of the cold crystallization, melting peaks are asymmetric because some small crystals melt while crystallization is still going on. At scan rate higher than 20 K min^{-1} all thermal effects become progressively less intense. Melting of TRE_α is always evident but becomes broader and, due to the short time needed to reach high-temperatures, only a limited amount of 'undercooled liquid' can undergo cold crystallization, as can be seen from the associated heat flow

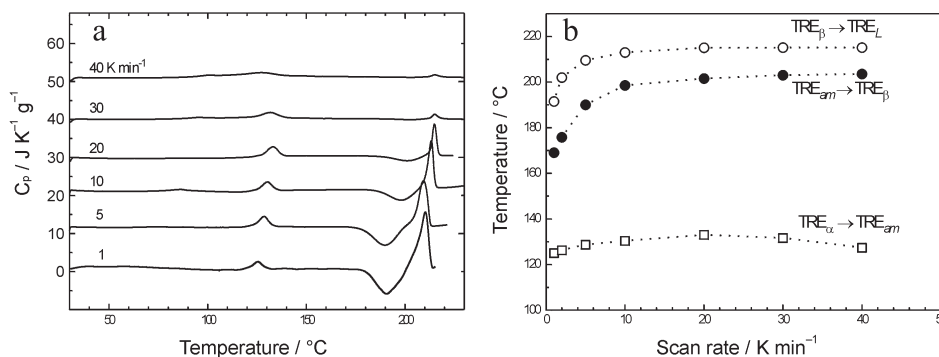


Fig. 2 Traces of DSC curves of TRE_{α} at different scan rate (from 1 to 40 $K min^{-1}$). Three thermal events are shown: melting of TRE_{α} , cold crystallization and subsequent melting of TRE_{β} (a); Dependence of the transition temperatures (peak) of TRE_{α} as a function of scan rate. Data refer to melting of TRE_{α} (\square), cold crystallization (\bullet) and to final melting of TRE_{β} (\circ), (data from Fig. 2a) (b)

which decreases asymptotically with the scan rate; as a consequence, the TRE_{β} melting peak height also becomes increasingly smaller. Given the non-equilibrium nature of the transformations, the values of the thermodynamic parameters for the transitions described are obviously functions of the scan rates, as can be seen from the data reported in Figs 2a and 2b.

Trehalose beta

This crystalline anhydrous form TRE_{β} was always prepared by exposing the starting dihydrate trehalose TRE_h to temperatures of above 130°C in an oven. The results from the calorimetric experiments carried out on TRE_{β} samples (Fig. 3a) show that there is only a very slight (if any at all) influence of the scan rate (from 1 to 40 min^{-1}) on their thermal behavior. No further thermal effects or deviations from the baseline are seen before temperatures close to 200°C, where the melting peak in the heat flow curve appears. The onset of the melting peaks is seen at slightly different temperatures, depending on the scan rate used.

However, for the DSC curves recorded at low scan rates (1 to 5 $K min^{-1}$), there is always a more or less pronounced shoulder in the lower temperature range of the melting endotherm. This shoulder disappears as the scan rate is increased and, in parallel, the transition becomes sharper. The presence of a trailing shoulder can easily be explained by considering the morphological factors influencing the melting temperature. The finite size of the crystals, their state of perfection and the presence of interfacial regions are the most common reasons for changes in the melting profiles. Quite obviously, dihydrate crystals subjected to a very rapid change in temperature, from 30 to 130°C, form new TRE_{β} crystals which are non homogenous in size, shape and perfection. Upon heating at relatively slow heating rates, the less perfect crystals melt

at lower temperature; while the specimen is still undergoing heating, there is enough time for a re-crystallization process with the final melting of both the new crystals and the already formed, more-perfect ones, with the higher melting point. When the heating rate is fast, the narrow time window for the melting process does not allow sufficient time for the recrystallization of the smaller, imperfect crystals and therefore they melt in the same temperature range as the bigger and more perfect ones, giving rise to a broader endotherm. The peak temperatures and the enthalpy values for the melting of TRE_{β} as a function of the heating rate are reported in Fig. 3b.

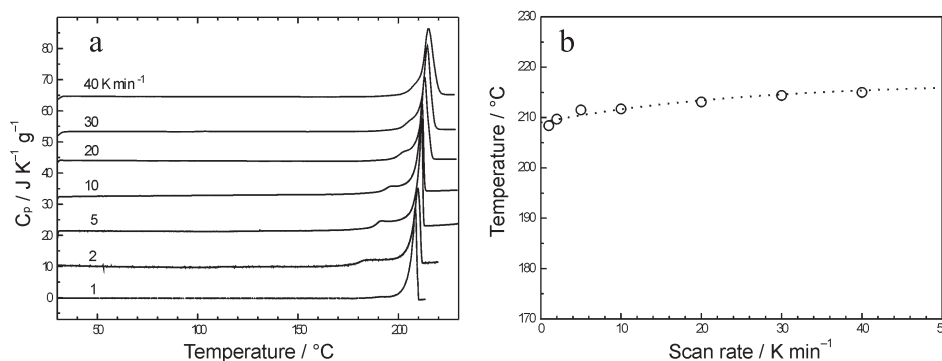


Fig. 3 Traces of DSC curves of TRE_{β} at different scan rate (from 1 to 40 K min⁻¹). Only the thermal events of melting with a pre-melting at low scan rates are evident (a); Dependence of the transition temperatures (peak) of TRE_{β} as a function of scan rate (data from Fig. 2a) (b)

The liquid phase after the melting of TRE_{β} was cooled at several scan rates, from 20 to 0.2 K min⁻¹ in order to crystallize TRE_{β} on cooling. The experiments were unsuccessful, even at the lowest cooling rate no crystallization was seen, which was attributed to the high viscosity of the liquid that hinders the formation of the new phase (the nucleation of the crystals within the liquid) and its growth.

Trehalose gamma

TRE_{γ} , the form reported for the first time by Sussich *et al.*, is composed of two domains, one dihydrate and one anhydrous, presumably an external layer of anhydrous crystal and an internal core of hydrated material.

The DSC trace shows a first endotherm around 125°C and a second endothermic peak, associated with the melting of the anhydrous TRE_{β} form (Fig. 4a), at much higher temperature. After the first thermal event, there are no signs of crystallization in the C_p curve before the peak at 230°C. This is taken as an evidence that the endotherm at lower temperature is a solid–solid transition, that is, a direct transformation of the hydrated part of TRE_{γ} to the TRE_{β} form, not going through a melting–recrystallization process. The main confirmation of this direct transformation comes from the X-ray powder diffraction pattern recorded as a function of tempera-

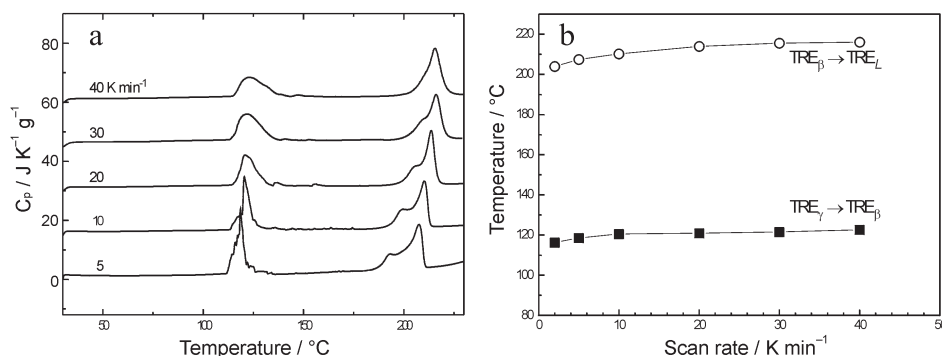


Fig. 4 Traces of DSC curves of TRE_γ at different scan rate (from 1 to 40 K min⁻¹). Solid–solid transition and melting of TRE_β are shown (a); Dependence of the transition temperatures (peak) of TRE_γ as a function of scan rate. Data refer to solid–solid transition of TRE_γ to TRE_β (■) and to final melting of TRE_β (○), (data from Fig. 4a) (b)

ture by using the Synchrotron radiation at the Elettra-Austrian-SAXS beamline with the SAXS/WAXS set-up (Sussich *et al.*, in preparation). However, verification of the interpretation also comes from DSC results alone. The TRE_γ form was heated at 20 K min⁻¹ above the transition temperature (about 140°C) and then, after quenching to room temperature, the sample was heated again at 20 K min⁻¹ up to 230 °C. A curve corresponding only to the melting of TRE_β was obtained, thus corroborating the above hypothesis.

We wish, however, to point out that the interpretation of the TRE_γ morphology implies a structural modification with some subtle metastable (non-equilibrium) state. That is, since the hydrated part of TRE_γ cannot be in an equilibrium state (TRE_h ‘melts’ at 100°C), the observed transition may not be considered a pure ‘thermodynamic’ transition. Therefore, it is rather surprising that this transition temperature does not change very much by varying the scan rate (Fig. 4b), while the sharpness of the transition peak increases at low scan rates, as it is expected for solid–solid transition at equilibrium.

In conclusion, the transition obtained for TRE_γ is a solid–solid one, although it does not seem to occur at equilibrium. Reproducible values have been obtained for this transition (temperature and enthalpy) and therefore included in Table 2. Changes in other properties (e.g. dV/dT) and the detailed investigation of its structural features will serve to explain the apparent discrepancy described above.

Enthalpies of transition

Despite the straightforward evaluation of the heats of transition from DSC studies, the data available in literature appear very scarce. Not only is the enthalpy of the transformation therefore missing, but also, as a consequence, no any further knowledge is available about the variation of interactions (energy and entropy changes) during the transition process.

Determination of transition enthalpies has been made on all the curves carried out at different scan rates. It was noted previously [10] that a large variation of the enthalpy of transition was found for the dehydration process with increasing scan rates up to a scan rate of about 10 K min^{-1} . No major variations of enthalpy changes were observed above this value of scan rate for the dehydration transition or for any other transitions throughout all the range of scan rates explored. Some scattering of the enthalpic data is observed, especially for the transition $\text{TRE}_\gamma \rightarrow \text{TRE}_\beta$. This has to be ascribed both to the difficulty of reproducibility in the preparation of the crystalline phase and to a possible underlying dependence of the enthalpy change with the scan rate.

All these data, integrated with some of the previously reported enthalpies of dehydration [10], are collected in Fig. 5. The trend of the data clearly shows that only for the dehydration process does the mechanism of transition change from low to high scan rate. Having previously [11] assessed that the transition $\text{TRE}_h \rightarrow \text{TRE}_\gamma$ is only a preliminary step before the full transformation into TRE_β , it turns out that the sum of the two thermal effects should be constant if the whole process is always that of dehydration with the final formation of TRE_β . This is shown by the dotted line (marked $\text{TRE}_h \rightarrow \text{TRE}_\beta$) in Fig. 5. A summary of the calorimetric data for the enthalpy of the several transitions, including the previous literature data of Roos [15] and of Sussich *et al.* [10], has been made by critical evaluation of the data and is reported in Table 2. This table also contains the entropy changes for the reported transitions, by using the values of the transition temperatures reported (as 'onset' values, as recommended by the IUPAC Working Group for calibration of calorimeters, see also [20]). The high value of the ΔS for the dehydration transition must be mostly attributed to the vaporization of the two water molecules contained in the crystalline lattice of TRE_h , for which the literature gives $108.8 \text{ J K}^{-1} \text{ mol}^{-1}$ [21]. The small value of ΔS cal-

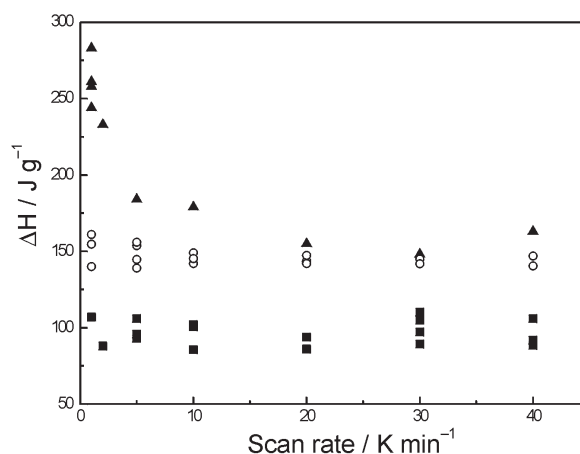


Fig. 5 Dependence of the enthalpy of transition as a function of scan rate for the dehydration process (▲), for the solid–solid transition of TRE_γ to TRE_β (■) and final melting of TRE_β (○)

culated for the amorphization of TRE_{α} reflects the high energy content (and the low ordering) of this structure. The ΔS for the solid–solid transition of TRE_{γ} would appear more surprising, if the relevant information of the presence of water still entrapped in its core is not taken into account.

Discussion

The scenario opened by the dehydration of trehalose TRE_h appears much more complex than originally thought from studies aimed mainly at the amorphization of the dihydrate crystals TRE_h . We would like to go, although superficially, through some of the issues that are of paramount importance for further investigations and understanding of trehalose action. Of course, the existence of polymorphs which interconvert to each other with a kinetic control is the interpretative key reported since our first study [10]. Among various transformations which have been reported here, we wish to emphasize specifically the role that these species may have in the still unraveled mechanism of cell protection in a dormant life.

It has been reported [19] that the process of vitrification upon the dehydration of a hydrate crystal may occur by ‘nucleation and growth of the amorphous phase, in an intriguing inversion of the familiar process of crystallization of metastable liquids’. This prompted us to re-examine, carefully, the conditions under which trehalose has been vitrified by water loss from its crystalline dihydrate. In particular, we have looked at the conditions necessary to obtain the metastable, fully anhydrous crystalline phase, which, according to Ding *et al.* [19], might be generated by using lower temperatures and powdered crystals. These authors reported that they were unable to prepare this form, here called TRE_{α} , while a careful scrutiny of their DSC curves reveals the typical transition of TRE_{α} crystals, obtained by dehydrating the TRE_h form at 70°C for 3 days (ca 5 torr). However, their first heating scan was assigned to a ‘re-equilibration above T_g of a glass of unusually low enthalpy’. Indeed, subsequent scans give the curves expected for glass transition and annealing treatments. X-ray diffractograms of TRE_{α} obtained by gentle dehydration procedure have been shown by Sussich *et al.* [9, 10] that TRE_{α} is quite crystalline although it cannot be obtained as a single crystal. This re-interpretation that the dehydration of TRE_h produces either amorphous or crystalline phases is important in view of the hypotheses for its protective action. Aldous *et al.* [22] have already proposed that this action involves the dihydrate crystallizability as a key feature and the T_g of the residual glass only secondarily. We would like to point out that a kinetic study of the water removal from the TRE_h form is being carried out with the support of a molecular dynamics simulation of the dehydration process, in order to verify Angell’s, conjecture that if the removal of water could produce a crystal with mechanical instability, then relatively low kinetic barriers would occur.

Conclusions

The data summarized here define the stability and inter-conversion temperatures of the various polymorphs of trehalose. Some of these findings may explain the discrepancies in literature results and interpretations, especially when the experimental conditions are not given in detail. As a corollary to the above discussion on the accurate knowledge of the different trehalose forms, it should be mentioned, for example, that X-ray powder patterns of amorphous trehalose reported in literature [19, 22, 24] do not agree quantitatively with each other. In addition, it may be worth noting that the solubility diagrams are not always in good agreement either (Fig. 1, [23]), not only because of the different methods used to approach the solubility 'equilibrium' but perhaps also because of the interference of anhydrous and hydrate crystalline phases. Given the correlations between the hydration properties of trehalose in solution and the structure of dihydrate crystals, our attention has focussed on the thermodynamics and the kinetics of water depletion from the dihydrate trehalose crystals, with the aim of filling this knowledge gap at molecular level (Sussich *et al.*, in preparation). Our long-range goal is to collect evidence for the role of the complex trehalose-water equilibria in the solid and in liquid phases during the cryptobiosis processes.

* * *

The authors would like to thank Prof. H. Suga and Prof. J. W. Brady for many helpful discussions. Financial support of MURST (COFIN-98) and of University of Trieste is also acknowledged.

References

- 1 C. A. Angell, *Science*, 267 (1995) 1924.
- 2 Y. H. Roos, 'Phase Transition in Foods', Academic Press, San Diego 1995.
- 3 E. Yu. Shalaev and F. Franks, *J. Chem. Soc. Faraday Trans.*, 91 (1995) 1511.
- 4 Y. H. Roos, *Food Technology*, 49 (1995) 97.
- 5 F. Franks, *Eur. J. Pharmac. Biopharmac.*, 45 (1998) 221.
- 6 L. M. Crowe, R. Mouradian, J. H. Crowe, S. A. Jackson and C. Womersley, *Biochim. Biophys. Acta*, 769 (1984), 141.
- 7 J. H. Crowe, L. M. Crowe and D. Chapman, *Science*, 223 (1984) 701.
- 8 W. Q. Sun and P. Davidson, *Biochim. Biophys. Acta*, 1425 (1998) 235.
- 9 F. Sussich, R. Urbani, A. Cesàro, F. Princivalle and S. Bruckner, *Carbohydr. Letters*, 2 (1997) 403.
- 10 F. Sussich, R. Urbani, F. Princivalle and A. Cesàro, *J. Am. Chem. Soc.*, 120 (1998) 7893.
- 11 F. Sussich, F. Princivalle and A. Cesàro, *Carbohydr. Res.*, 322 (1999) 113.
- 12 H. J. Reisener, H. R. Goldschmid, G. A. Ledingham and A. S. Perlin, *Canad. J. Biochem. Physiology*, 40 (1962) 1248.
- 13 T. Chen, A. Fowler and M. Toner, *Cryobiology*, 40 (2000) 277.
- 14 F. Shafizadeh and R. A. Susott, *J. Org. Chem.*, 38 (1973) 3710.
- 15 Y. H. Roos, *Carbohydr. Res.*, 238 (1993) 39.
- 16 Y. H. Roos, *J. Thermal Anal.*, 48 (1997) 535.
- 17 L. Slade and H. Levine, *Crit. Rev. Food Sci. Nutr.*, 30 (1991) 115.

- 18 J. L. Green and C. A. Angell, *J. Phys. Chem.*, 93 (1989) 2880.
- 19 S. P. Ding, J. Fan, J. L. Green, Q. Lu, E. Sanchez and C. A. Angell, *J. Thermal Anal.*, 47 (1996) 1391.
- 20 G. Della Gatta (Ed.), Special Issue on Calibration of Calorimeters, *Thermochim. Acta*, 347 (2000) 9–13 and 85.
- 21 D. Eisenberg and W. Kauzmann, *The Structure and Properties of Water*, Oxford Univ. Press 1969, p. 98.
- 22 B. J. Aldous, A. D. Auffret and F. Franks, *Cryo Letters*, 16 (1995) 181.
- 23 D. P. Miller, J. J. de Pablo and H. Corti, *Pharmaceutical Research*, 14 (1997) 578.
- 24 H. Suga, personal communication.